Biophysical Journal, Volume *110*

Supplemental Information

Conformational Mobility in Cytochrome P450 3A4 Explored by Pressure-Perturbation EPR Spectroscopy

Dmitri R. Davydov, Zhongyu Yang, Nadezhda Davydova, James R. Halpert, and Wayne L. Hubbell

Cytochrome P450 3A4 transitions revealed in a pressure perturbation study by LRET and EPR spectroscopy

Dmitri R. Davydov, Zhongyu Yang, Nadezhda Davydova, James R. Halpert[1] and Wayne L. Hubbell

Supplemental Material

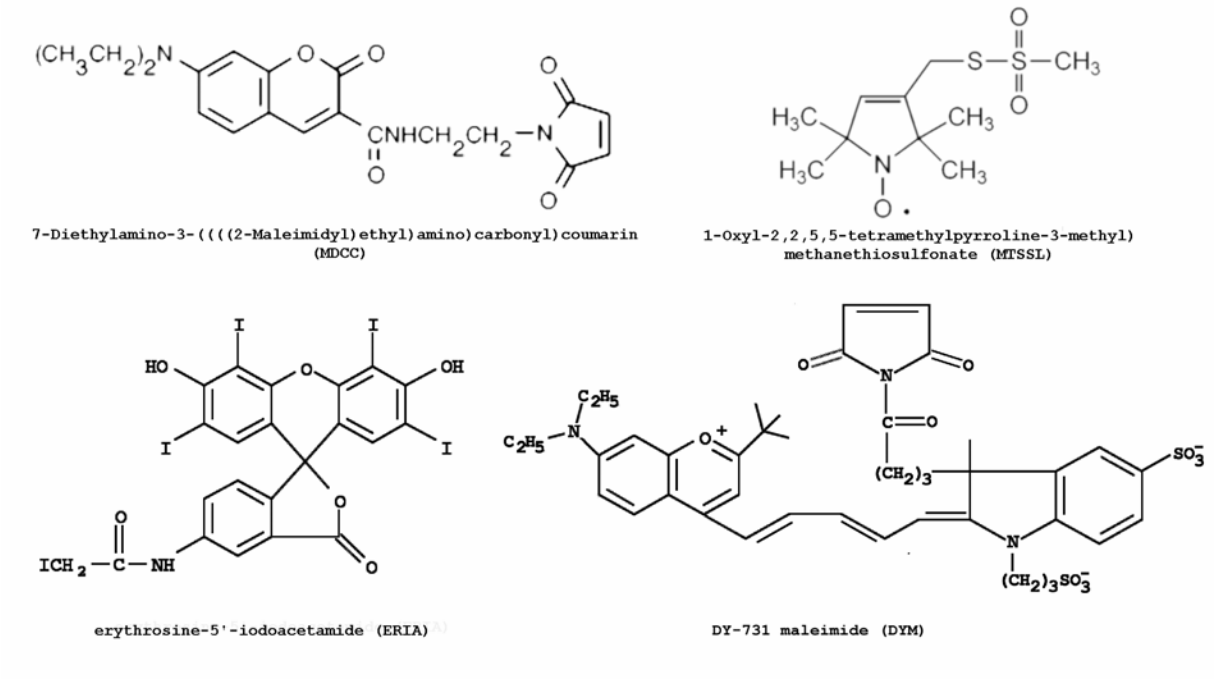

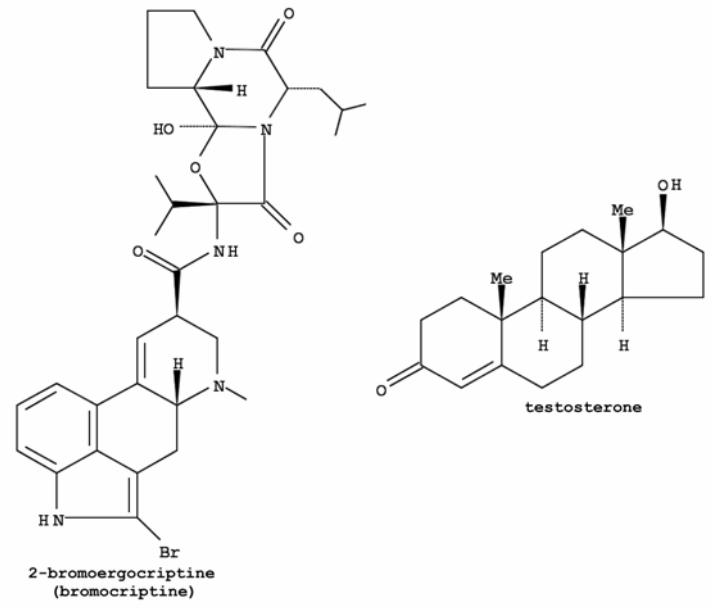

Fig. S1. Structures of thiol-reactive probes and CYP3A4 substrates used in this study.

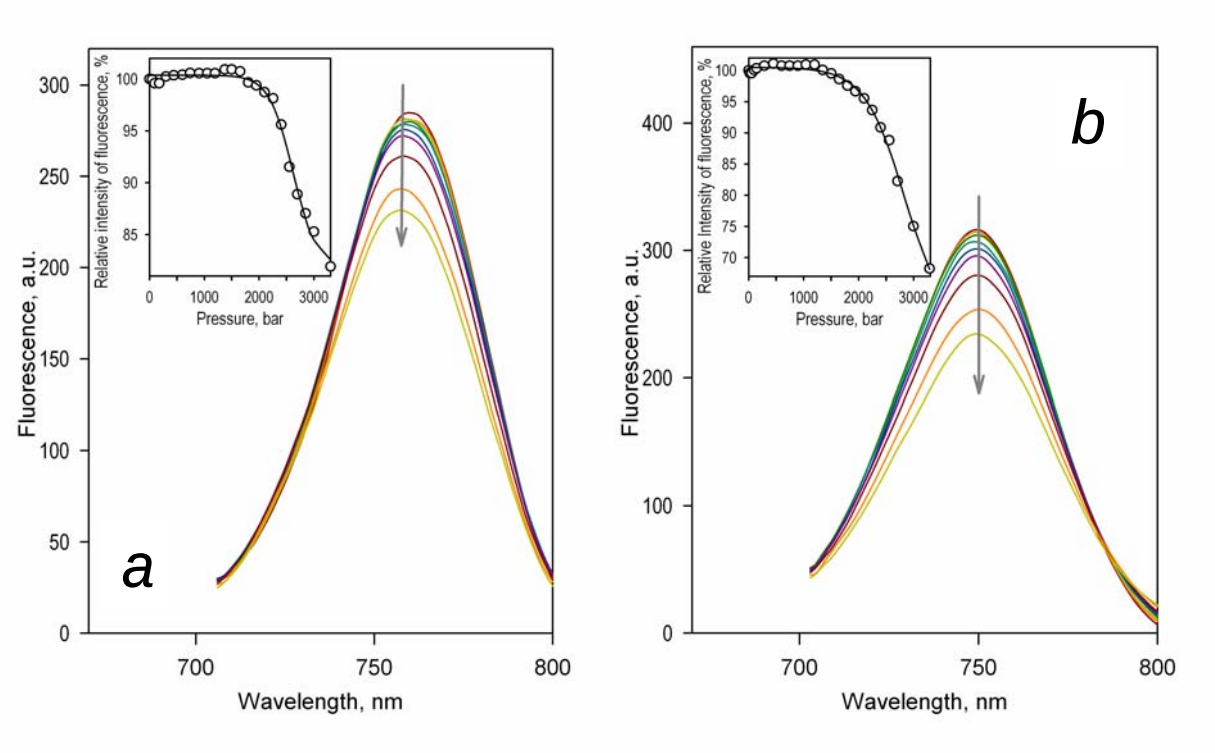

Fig. S2. Effect of pressure on fluorescence of DY-731 CYP3A4(C64,C468)-ERDY with no ligand added (***a***) and in the presence of 200 µM testosterone (***b***). The spectra shown in the figure correspond to pressures increasing from 1 to 3000 bar with a 300 bar increment. The insets show the pressure dependencies of the relative intensity of fluorescence. Conditions: 10 µM CYP3A4(C64,C468)-ER/DY in 0.1 M Na-Hepes buffer, pH 7.4, 4 °C. The spectra were recorded with direct excitation of DY-731 fluorescence with the use of a laser diode emitting at 650 nm. As seen from this figure, there were virtually no changes in the fluorescence intensity observed at the pressures below 2000 bar. The changes observed in these pressure range were limited to some minor broadening of the emission band, which was reversible upon decompression (not shown). The gradual decrease in fluorescence of DY-731 observed at higher pressures was irreversible and associated with an insignificant (<1 nm) blue shift of the emission band. Fitting of the pressure dependencies with Eq. 4 (insets, solid lines) suggests that the apparent pressure-induced denaturation of the protein revealed in these changes in the absence of ligand is characterized by the values of $\Delta V°$ and $P_{½}$ of -107 ml/mol and 2615 bar. The respective values determined in the presence of testosterone are equal to -63 ml/mol and 2836 bar.

.

Table S1. Properties of the single-cysteine mutants of CYP3A4 and their MDCC- and MTSSL-labeled derivatives used in this study*

Protein	F_{HS}, % [a]	F_{P420}, % [b]	Interactions with testosterone [c]		
			S_{50}, μM	N_H	$\Delta F_{HS,max}$, %
CYP3A4WT	16.2 ± 3.6	3.1 ± 6.1	55.6 ± 12.0	1.10 ± 0.12	32.5 ± 5.9
C64	21.2 ± 7.9	19.2 ± 14.5	76.7 ± 13.4	1.26 ± 0.34	22.7 ± 13.3
C64-MDCC	10.2 ± 14.9	23.1 ± 20.3	62.1 ± 19.5	1.25 ± 0.06	21.1 ± 2.7
C64-R1	11.8 ± 3.0	30.7 ± 14.9	88.7 ± 7.8	1.19 ± 0.11	14.0 ± 0.4
C85	17.9 ± 2.5	24.0 ± 11.4	70.1 ± 37.7	1.08 ± 0.12	14.9 ± 0.6
C85-MDCC	20.5 ± 4.7	16.8 ± 5.1	81.7 ± 8.3	1.12 ± 0.18	15.1 ± 0.3
C85-R1	12.9 ± 1.4	33.2 ± 2.9	73.8 ± 7.1	1.18 ± 0.05	12.7 ± 1.3
C98	24.2 ± 7.2	11.9 ± 23.3	76.5 ± 4.7	1.15 ± 0.07	18.8 ± 0.4
C98-MDCC	22.8 ± 2.3	2.7 ± 1.8	90.9 ± 14.7	1.36 ± 0.43	17.6 ± 15.3
C98-R1	13.4 ± 0.4	17.3 ± 0.6	57.3 ± 5.4	1.01 ± 0.03	30.5 ± 1.6
C121	13.6 ± 4.6	11.3 ± 9.9	92.5 ± 3.8	1.11 ± 0.27	4.6 ± 0.6
C166	19.7 ± 2.8	18.6 ± 8.3	80.1 ± 16.1	1.30 ± 0.18	20.8 ± 5.1
C166-MDCC	24.6 ± 4.0	16.5 ± 10.8	90.8 ± 0.0	1.13 ± 0.14	23.9 ± 0.4
C166-R1	7.2 ± 1.7	52.5 ± 0.9	76.0 ± 8.8	1.14 ± 0.27	13.2 ± 2.7
C343	14.3 ± 4.0	47.1 ± 1.8	72.4 ± 4.2	1.05 ± 0.06	50.2 ± 1.0
C343-MDCC	19.5 ± 3.5	41.0 ± 5.4	36.0 ± 4.4	1.41 ± 0.22	18.7 ± 0.7
C343-R1	13.3 ± 0.1	43.2 ± 2.4	62.7 ± 6.3	1.05 ± 0.11	20.5 ± 6.1
C409	28.4 ± 10.8	11.6 ± 6.8	59.5 ± 6.6	1.16 ± 0.28	33.1 ± 1.8
C409-MDCC	4.6 ± 1.3	43.9 ± 6.6	60.5 ± 23.3	1.11 ± 0.28	32.0 ± 8.9
C409-R1	14.3 ± 2.6	20.6 ± 2.9	70.1 ± 9.4	1.00 ± 0.04	29.1 ± 2.6
C468	28.1 ± 10.6	7.1 ± 2.8	76.9 ± 13.5	1.15 ± 0.19	25.2 ± 2.4
C468-MDCC	11.1 ± 3.0	7.6 ± 0.5	74.6 ± 9.0	1.66 ± 0.02	13.3 ± 1.9
C468-MTSL	26.4 ± 0.5	6.5 ± 1.2	72.4 ± 7.5	1.30 ± 0.26	21.8 ± 11.2
C495	25.0 ± 7.0	7.2 ± 5.0	ND	ND	ND
C495-MDCC	26.1 ± 4.1	31.0 ± 1.9	86.5 ± 6.3	1.04 ± 0.08	20.9 ± 0.6

* The values given in the Table represents the averages of the results of 2-6 individual measurements. The "±" values show the confidence interval calculated for $p = 0.05$.

[a] Fraction of the high-spin state as related to the total CYP3A4 content.

[b] Fraction of apparent P420 state as related to the total CYP3A4 content.

[c] Parameters of interactions of CYP3A4 variants with testosterone determined from fitting of the dependencies of the high-spin content on testosterone concentration (0 – 500 μM) to the Hill equation. Conditions: 0.1 M Na-Hepes buffer pH 7.4, 25 °C, 1.5 – 2 μM protein. $\Delta F_{HS,max}$ represents the limiting amplitude of the substrate-induced transition as determined from the fitting.

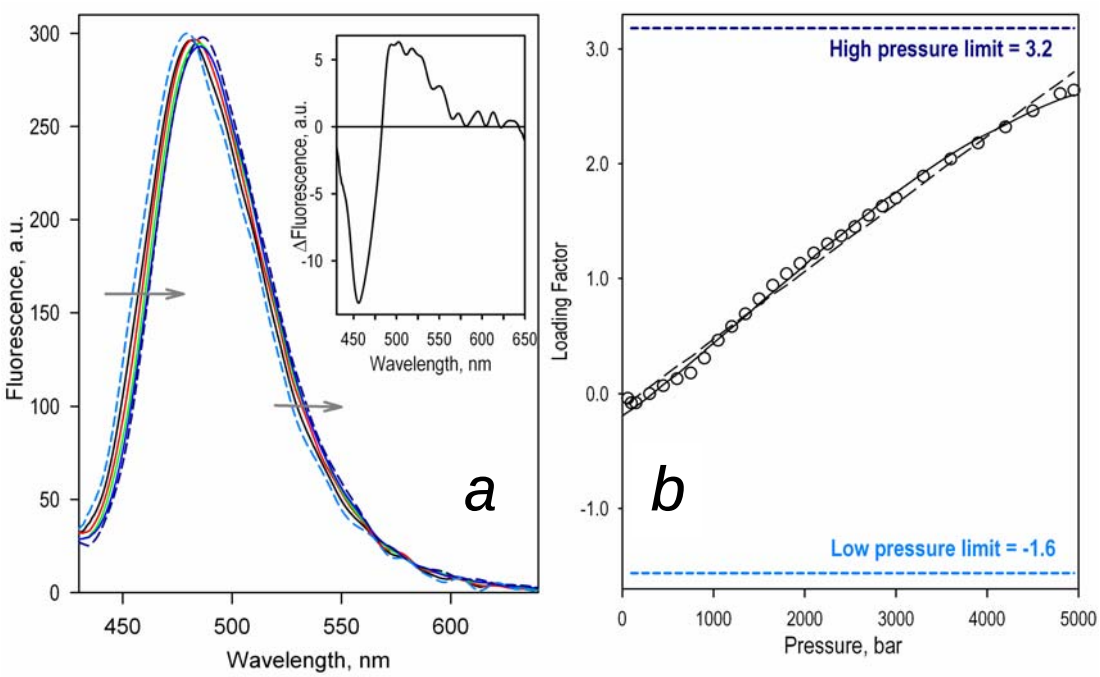

Fig. S3. Pressure-induced changes in fluorescence of MDCC-GSH adduct in solution and reconstruction of the spectra of fluorescence characteristic to the apparent low- and high-pressure end states of the fluorophore. Spectra shown in solid lines in panel ***a*** were recorded at 1 (black), 1800 (red), 3600 (green), and 4900 bar (blue). Inset shows the spectrum of the first principal component found by PCA. The dashed lines show the spectra of the low-pressure (light blue) and high-pressure (dark blue) end states reconstructed based on approximation of the pressure dependence of the loading factor (panel ***b***) to equation 4, which is shown in solid line. The values of $\Delta V°$, $P_{½}$, A_0 and A_{max} found from this approximation are equal to -14.4 ml/mol, 1549 bar, -1.6 and 4.7 respectively (ρ^2=0.998). Thick dashed lines on panel ***b*** show the limiting levels of the loading factor dictated by the values of A_0 and A_{max}. Thin dashed line on panel ***b*** corresponds to a linear approximation of the same data set (ρ^2=0.992), which is shown for comparison. The spectra shown in dashed lines in panel ***a*** were obtained by adding the spectrum of the 1st principal component (panel ***a***, inset) multiplied by the low-pressure (light blue) or high-pressure (dark blue) limit level (-1.6 and 3.2, respectively) to the spectrum taken at 1 bar.

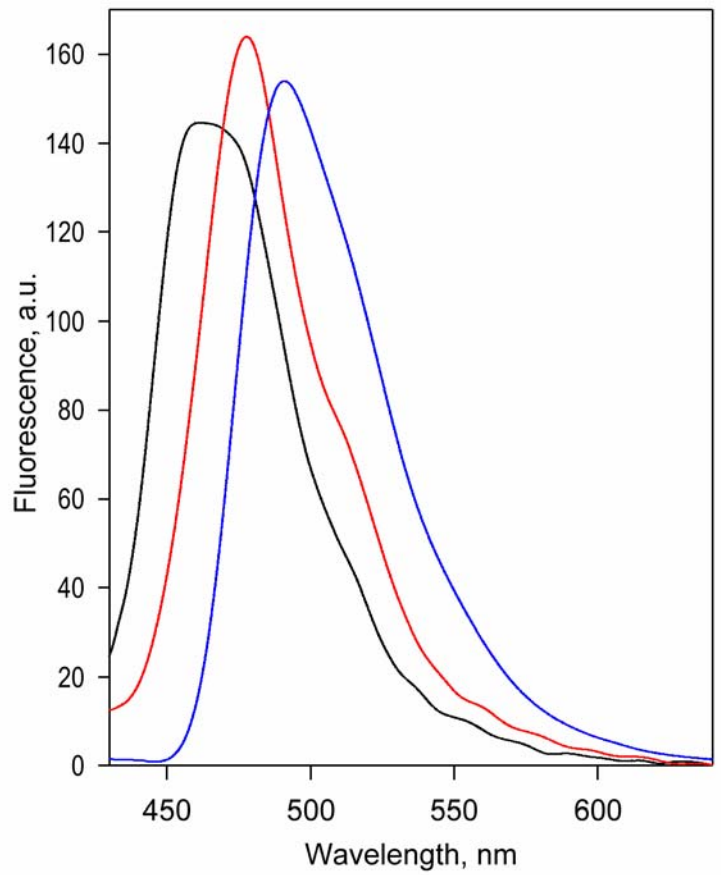

Fig. S4. A set of prototypical spectra of fluorescence of MDCC used in the analysis of pressure-induced changes of fluorescence of MDCC-labeled single-cysteine mutants of CYP3A4. The spectra shown in red and blue, which correspond to the apparent low-pressure and high-pressure (blue) states of water-exposed label respectively, were obtained by averaging the results of three individual experiments on the effect of pressure on fluorescence of MDCC-GSH adduct (see Fig. S2). The spectrum shown in black corresponds to the apparent low-pressure end-state of the buried protein-bound label. This spectrum was obtained with a procedure similar to that illustrated in Fig. S2 applied to a series of spectra of CYP3A4(C409)MDCC *vs*. pressure.

It should be noted that the sole purpose of the use of this set of basis spectra in our interpretation of the observed changes in terms of pressure induced displacement of the equilibrium between states with different position of the emission band is to better reveal their physical nature. This approximation has no effect on the deduced parameters of the transition, which were obtained from the pressure dependence of the loading factor for the first principal component and were therefore model-independent.

Implementation of Principal Component Analysis in the Analysis of Pressure-Induced Changes in EPR Spectra of Protein-Incorporated Paramagnetic Probes

Principal Component Analysis (PCA), which is sometimes also termed as “bilinear factor analysis”, was first introduced in chemistry by Malinowski (Malinowski 1980). Briefly, this approach is based on the analysis of a covariance matrix built from a series of spectra reflecting the course of chemical transitions in the system induced by some independent variable (Z), such as time, temperature, pressure, etc. PCA makes it possible to compile the most representative changes in the system into a limited number of so-called principal components each characterizing an individual abstract transition taking place in response to changing Z. Each principal component is represented by a respective eigenvector, which may be thought of as a difference spectrum of the transition, and a set of eigenvalues (loading factors), each characterizing the amplitude of the respective transition at each of the Z values in the experimental dataset. PCA and Singular Value Decomposition (SVD), which represent two closely related techniques implementing different formalisms, are the techniques of choice for the analysis of changes in the spectra of absorbance and fluorescence of complex systems (Ross 1995; Hendler 1994; Tam 1994).

In our implementation, PCA is applied to the matrix $\boldsymbol{D}_{\mathrm{exp}}$ formed by the differential spectra obtained by subtracting the first spectrum of the series (the spectrum taken at ambient pressure) from each consecutive spectrum. According to the fundamentals of PCA (Ross 1995; Hendler 1994), this matrix is represented as:

$$\boldsymbol{D}_{\mathrm{exp}} = \boldsymbol{A}\boldsymbol{B}^{\mathrm{t}}$$

Here $\boldsymbol{A}$ is the matrix of the eigenvectors, which may be interpreted as the differential spectra corresponding to each of the abstract transitions found by PCA, and $\boldsymbol{B}$ is the matrix of the respective loading factors (eigenvalues) that characterize the apparent depth of the abstract transitions at each experimental point. A major difficulty with interpretation of the results of PCA is that the experimental data can be fit equally well with an infinite aggregate of linear combinations of the columns of the matrices $\boldsymbol{A}$ and $\boldsymbol{B}$ (Ross 1995; Tam 1994). Generally speaking the matrices $\boldsymbol{A}$ and $\boldsymbol{B}$ represent some linear transforms of the matrices $\boldsymbol{A}_{\mathrm{p}}$ and $\boldsymbol{B}_{\mathrm{p}}$ corresponding to the real, physically relevant transitions. The matrix $\boldsymbol{B}_{\mathrm{p}}$ may be thought as being a product of matrix $\boldsymbol{B}$ and the transformation matrix $\boldsymbol{T}$:

$$\boldsymbol{B}_{\mathrm{p}} = \boldsymbol{B}\boldsymbol{T} \tag{4}$$

If the transformation matrix $\boldsymbol{T}$ is known, the matrix $\boldsymbol{A}_{\mathrm{p}}$ that represents the differential spectra characteristic to each of the individual physically-relevant transitions may be found as:

$$\boldsymbol{A}_{\mathrm{p}} = \boldsymbol{A}(\boldsymbol{T}^{-1})^{\mathrm{t}} \tag{5}$$

This formalism constitutes the basis of target factor analysis (TFA) (Tam 1994). In this approach the idealized prototype of matrix $\boldsymbol{B}_{\mathrm{p}}$ is built on the basis of some known or hypothetical functional dependencies of the physically-relevant underlying transitions on variable parameter (e.g., pressure, time, temperature, etc.). Approximation of the calculated target functions with linear combinations of the rows of matrix $\boldsymbol{B}$ (dependencies of the loading factors on variable parameter) allows one to build matrix $\boldsymbol{T}$ and then find the hypothetical representations of the matrices $\boldsymbol{B}_{\mathrm{p}}$ and $\boldsymbol{A}_{\mathrm{p}}$.

References.

Malinowski, E. R. and D. G. Hovery (1980). Factor Analysis in Chemistry. New York, Willey-Interscience.

Ross, R. T. and S. Leurgans (1995). Component resolution using multilinear models. *Biochem. Spectroscopy* **246**: 679-700.

Hendler, R. W. and R. I. Shrager (1994). Deconvolutions based on singular-value decomposition and the pseudoinverse - a guide for beginners. *J. Biochem. Biophys. Meth.* **28**(1): 1-33.

Tam, K. Y. and F. T. Chau (1994). Multivariate study of kinetic data for a 2-step consecutive reaction using target factor-analysis. *Chemometrics and Intelligent Laboratory Systems* **25**(1): 25-42.